Ab initio calculation of properties of carbon in the amorphous and liquid states

Giulia Galli* and Richard M. Martin
University of Illinois, Department of Physics and Material Research Laboratory, Urbana, Illinois 61801

Roberto Car
International School for Advanced Studies, Strada Costiera 11, 34014 Trieste, Italy

Michele Parrinello
IBM Research Division, Forschungslaboratorium Zurich, CH-8803 Ruschlikon, Switzerland and International School for Advanced Studies, Strada Costiera 11, 34014 Trieste, Italy
(Received 14 December 1989; revised manuscript received 2 April 1990)

We have carried out a detailed investigation of liquid carbon (*l*-C) at $T \simeq 5000$ K, and quenched amorphous carbon (*a*-C) at room temperature, using a first-principles molecular-dynamics method. In this paper we report calculations performed for a fixed density corresponding to low pressures. From our results, which agree well with the limited experimental information available, we analyze the short-range order, particularly the fractions of *sp*, sp^2, and sp^3 sites, and the electronic properties of the two systems. In addition, we discuss new features of *a*-C and *l*-C, predicted by our calculation, and present an analysis of some models proposed in the literature to account for their electronic and bonding properties, as well as of recent controversial experiments.

I. INTRODUCTION

The ability of carbon to have twofold, threefold, and fourfold coordination leads to a variety of bonded forms in both solid and liquid states, relevant to diverse fields of science and technology.[1-4] In recent decades, a widespread effort has been devoted to the understanding of the structural and electronic properties of metastable disordered carbon,[4-17] and systematic investigations have been carried out to characterize the nature of the liquid state[3,14,18-28] and the melting mechanism.[3,18,21-26,28,29] Nevertheless, outstanding questions concerning the physics of noncrystalline and liquid carbon(1-C) remain unanswered. Indeed, large uncertainties are involved in the experimental techniques and existing measurements have often led to controversial interpretations; furthermore, the ability of theoretical models and calculations to account for the complicated bonding properties of disordered carbon has so far been rather limited.

In this paper, we present detailed analyses of the structural and electronic properties of both amorphous and liquid carbon, which we have investigated[30] with a computer simulation based on a first-principles molecular-dynamics (MD) method.[31,32] Unlike conventional MD and Monte Carlo approaches, the interatomic potential is explicitly derived from the electronic ground state, which is treated with accurate density-functional techniques. This scheme, which has successfully been used for the simulation of a variety of systems (crystalline[33] and disordered[34] materials, and microclusters[35]), allows for the *ab initio* investigation of thermodynamical quantities and can account for the correlation between electronic and bonding properties, and atomic dynamics. Since density-functional (DF) theory[36] has proven to be a valuable tool for the investigation of different forms of C—such as diamond,[37] graphite,[38] high-pressure metallic phases,[39,40] and carbon molecules[41]—we propose that our calculations of the thermodynamic properties accurately treat the complex bonding characteristics of carbon, and give realistic predictions of unknown properties in the liquid and solid states.

A. Properties of disordered carbon

The field of disordered C covers a very wide range of systems: Carbon grains, composed of long-chain molecules and solid carbonaceous particles, present in interstellar molecular clouds and in certain cool old stars;[42] graphitic and diamond cluster mixtures, such as those recently found to be the main constituents of carbon detonation products in soot formation;[43] carbon fibers, chars, and cokes, involved as intermediate species in the pyrolisis of carbonaceous materials into graphite;[4(a)] glassy carbon (*g*-C), formed by heating organic polymers;[5] amorphous carbon (*a*-C), produced by sputtering or evaporation in an electron bean or carbon arc [Ref. 4(a)]; "diamondlike" films, obtained, e.g., by vapor deposition.[17]

The solid disordered materials *g*-C, *a*-C, and diamondlike phases may be classified according to their macroscopic densities (ρ_d). That of *g*-C ranges from 1 to 1.5 $g\,cm^{-3}$, whereas estimates of ρ_d for *a*-C indicate values between 1.8 and the graphic density (2.27 $g\,cm^{-3}$).[4(a)] Diamondlike films have, in general, densities intermediate between that of graphite and diamond (3.52 $g\,cm^{-3}$); however, some investigations indicate that superdense phases ($\rho_d \simeq 4$ $g\,cm^{-3}$) may also be present in these ma-

terials.[17] Among the many disordered forms of C, we restrict here our attention to *a*-C, and, in particular, to its local atomic structure and electronic properties.

From a technological point of view, this is a particularly attractive material: It combines semiconducting properties in some respect similar to graphite with a much higher hardness, and it exhibits characteristics distinct from those of other amorphous semiconductors, e.g., silicon, germanium, and chalcogenides, such as a higher electrical conductivity which increases as a function of temperature.[4] *a*-C films have been widely used as supports in electron microscopy, and have potential applications as tunneling barriers in electronic components and, in general, in the technology of switching and memory devices.

A question of primary interest regards the atomic structure of *a*-C; the determination of the fraction of sp^2:sp^3 sites is, in particular, a problem greatly debated in the literature and yet controversial. Estimates of sp^3 sites concentration ranging from 5 to 50 % have been obtained from radial distribution function analyses.[5–9] In very recent near-edge (NEXAFS) and extended (EXAFS) x-ray-absorption fine-structure studies,[10] a "graphitelike" fraction ranging from 60%, at $T=30\,^{\circ}\mathrm{C}$, to 90%, at $T=1050\,^{\circ}\mathrm{C}$, has been reported. These results are consistent with those of electron energy loss and $(e,2e)$ spectroscopy,[11] which indicate a sp^2 concentration of 85–100 % in evaporated *a*-C, and of 75–100 % in ion-sputtered *a*-C, at room temperature.

The knowledge of the liquid-state properties is less complete than that of the amorphous materials, despite a variety of investigations carried out in different fields, such as condensed-matter physics,[1] astrophysics,[2] and geology.[3,18] The key problem, of course, concerns the extreme temperatures ($T \geq 4000$ K) required to melt carbon. The phase diagram orginally proposed by Bundy,[18(a)] and investigations of the sixties and seventies,[18(b)] indicate the occurrence of a triple point in the high-T, low-pressure (P) regime, suggesting that *l*-C does not exist at atmospheric pressure. However, recent reports of graphite surface melting by high-energy laser pulses[19–21,23] have shown that there is at least a small range of T for which *l*-C can be obtained at low P. In particular, carbon has been shown to undergo a solid-liquid phase transition at $T=4450$ K and $P \leq 4$ bar.[21(a)] The high melting temperature of C is possibly related to the large defect formation energies (usually associated with a high enthalpy of fusion[44]) in both graphite[45] and diamond,[46] and to the large energy differences between graphite and diamond, and higher coordinated metallic phases,[39,40] compared, e.g., with the case of silicon.

The high-pressure and high-temperature regions of the C phase diagram, whose characterization is of the greatest importance in astrophysics and geology, are largely unknown. For example, whether carbon in outer planets such as Uranus and Neptune (where it is known to be at $P \simeq 6$ Mbar and $T \simeq 7000$ K) is solid or liquid[2] and which phases of C are present in the earth mantle (of crucial relevance to the understanding of mantle dynamics[3(a)]) are still open questions.

There have been no measurements which determine directly the structure of *l*-C, but only indications of structural transformations as graphite and diamond melt.[3(b),19-21] Speculations[3(c),24(a)] based on thermodynamics data depict the liquid in the low-P regime as a mixture of C_n chains, similar to those found in carbon vapors, with the simpler species C_1 and C_2 tending to gain in relative importance with raising T. According to the results of several spectroscopic investigations of graphite at high T, Whittaker and other authors[47,48] have proposed that graphite is not stable above 2600 K, at any pressure, but transform to the so-called "carbyne" solid, composed of chainlike structures containing triple bonds. If so, this would support the picture that liquid carbon is low coordinated, with *sp*-bonded carbon atoms. However, the existence of the carbyne region of the phase diagram has been often questioned in the literature of the past decade.[49] According to a model based on the empirical determination of graphite and diamond melting curves, Korsunskaya *et al.*[25] suggested that the melting of graphite is accompanied by the breaking of short-range covalent bonds and that, at low P, *l*-C consists mainly of neutral particles interacting via van der Waals forces. Ferraz and March[26] proposed a phenomenological description based on the Landau theory of phase transitions, which suggests that both an insulating and a metallic phase are present in the liquid, and, in particular, that at $P \simeq 2$ kbar a nonmetal-metal transition takes place between an *sp*-hybridized nonmetallic system with coordination 2 and a highly correlated liquid metal.

The electronic properties of *l*-C have also been the subject of theoretical and experimental controversies. One proposal that the liquid at low P is a semi-insulator has been supported by time-resolved reflectivity studies of graphite samples irradiated by intense laser pulses.[20] However, more recent optical and dc conductivity experiments[21] indicate that *l*-C is metallic, with a nearly temperature-independent electrical resistivity ($\rho_r = 30-70\ \mu\Omega\,\mathrm{cm}$). In other experiments,[27] pulse heating of *g*-C under pressure (4 kbar) has been shown to lead to a melt with a roughly constant ρ_r around 1 $m\Omega\,\mathrm{cm}$, for T up to 6000 K.

Evidence has been cited[24(a)] to show that the density of *l*-C is less than that of the solid at the triple point. An extrapolation from thermodynamical data of the graphite density at the triple point, and the somewhat arbitrary assumption of a volume expansion of 20%, gives an estimate of $\rho_d = 1.6\ \mathrm{g\,cm^{-3}}$ for *l*-C.[24(a)] A lower density, $\rho_d = 1.37\ \mathrm{g\,cm^{-3}}$, has been obtained from measurements of the void fraction and density of the recristallized graphite melt.[24(b)] On the other hand, the hypothesis that carbon behavior upon melting parallels that of the other group-IV elements, would indicate a density larger than that of graphite in the liquid phase at low P. A value of $\rho_d = 2.7\ \mathrm{g\,cm^{-3}}$, for example, has been proposed in the literature.[21(b)] As far as the liquid at high P is concerned, recent shock waves experiments[29] and transmission electron microscopy investigations of carbon melts[1,3(b)] seem to indicate that the diamond-liquid phase boundary has a positive slope, contrary to what has long been believed, and therefore a carbon liquid which is less dense than diamond.

B. Status of theoretical work

The ability of theoretical calculations to clarify the properties of amorphous and liquid carbon has been limited. Random network models (RNM) (Ref. 12) have been developed in order to understand the structure of noncrystalline carbons and tight-binding Hamiltonians[13] constructed to get insight into their electronic properties. Although useful, these approaches suffer the basic limitations of relying upon experimental inputs and *a priori* assumptions on certain characteristics of the network. Empirical potentials have recently been proposed,[14] which have a partial success in reproducing some structural properties of *a*-C and *l*-C. For example, in Ref. 14 the average coordination of the amorphous material is calculated to be less than 4.00, in agreement with experiment, whereas the liquid is found to have a coordination less than 3.00, which decreases as the temperature is raised in the range 6000–8000 K. The density of the liquid is determined to be 1.8 g cm^{-3} at $T \simeq 6000$ K and to decrease as well, as a function of T, indicating that the slope of the diamond-liquid phase boundary is positive. However, these empirical models fail to account for basic features of the physics of carbon, such as the layered structure of graphite and for the important interrelation between local atomic order and electronic structure. A realistic description of the different aggregation states of C appears to be crucial to the understanding of the properties of the disordered and liquid phases, for which atomic coordination plays a key role.

The rest of the paper is organized as follows: In Sec. II we describe our computational procedure; Secs. III and IV contain a discussion of our results for *a*-C and *l*-C, respectively. Finally, our conclusions and a brief description of work in progress are presented in Sec. V.

II. CALCULATION

A. Method

The key point is the first-principles MD method of Ref. 31 is the definition of a fictitious dynamical system whose potential energy surface is an appropriate functional of both ionic and electronic degrees of freedom: The former are the ionic (or ionic cores) coordinates ($\{R_I\}$) and the latter the single-particle orbitals of DF theory ($\{\psi_i\}$), treated within the local-density approximation (LDA). When this functional is minimized with respect to ($\{\psi_i\}$), one recovers the Born-Oppenheimer (BO) energy surface, to be used in MD simulations of the physical trajectories of the nuclei.

In more detail, a generalized classical Lagrangian is introduced:

$$\mathcal{L}_{eI} = K_e + K_I - E[\{\psi_i\},\{R_I\}] + \sum_{ij} \Lambda_{ij} \left[\int d\mathbf{r} \psi_i^*(\mathbf{r}) \psi_j(\mathbf{r}) - \delta_{ij} \right] \quad (1)$$

which yields the following coupled equations of motion for $\{R_I\}$ and $\{\psi_i\}$:

$$\mu \ddot{\psi}_i = -\frac{\delta E}{\delta \psi_i^*} + \sum_{j=1,N} \Lambda_{ij} \psi_j \ , \quad (2)$$

$$M_I \ddot{\mathbf{R}}_I = -\nabla_{\mathbf{R}_I} E \ , \quad (3)$$

$K_e = \mu \int d\mathbf{r} |\dot{\psi}|^2$ is a classical kinetic energy term associated with the $\{\psi_i(\mathbf{r})\}$, where μ is a parameter of dimension mass times length squared; $K_I = \sum_I \frac{1}{2} M_I \dot{R}_I^2$ is the kinetic energy of the ions of masses M_I. Λ_{ij} are Lagrange multipliers that impose the orthonormality constraints between the N occupied single-particle orbitals. $E[\{\psi_i\},\{R_I\}]$ is given by the sum of an electronic part, the Hohenberg-Kohn energy functional,[36] and of an ionic part corresponding to the direct Coulomb interaction of the ions in a uniform negative background.

For arbitrary values of the parameter μ and of initial conditions $\{\psi_i\}_0\{\dot{\psi}_i\}_0$, thermal equilibration between the classical degrees of freedom $\{R_I\}$ and $\{\psi_i\}$ will be achieved, after some time, by equipartition. If μ and $\{\psi_i\}_0\{\dot{\psi}_i\}_0$ can be chosen so that the two sets of degrees of freedom are only weakly coupled, the transfer of energy between them is small enough, to allow the electrons to follow adiabatically the ionic motion, remaining close to their instantaneous BO surface. In such a metastable situation, the time for thermal equilibration is considerably larger than characteristic ionic relaxation times, and therefore meaningful temporal averages can be computed.[30,32–35] In the case of metallic systems, we have found[30] that the time scales of the electronic and ionic motion may become comparable and thermal equilibration occur within fairly small-time intervals. In particular, metals at high temperature present special problems due to the broad spectrum of ionic characteristic frequencies. Statistical averages can still be computed if the electronic coordinates can be kept close to their BO surface.

We have developed a suitable scheme for the computation of thermodynamical properties of metals, in which a constant-volume–constant-temperature (CVT) MD technique is used. Following the formulation suggested by Nosé[50] for conventional MD, we define a Lagrangian $\mathcal{L}$ for an interacting system of electrons and ions, with the ions only in thermal equilibrium with an external heat reservoir of fixed temperature T_{ext}:

$$\mathcal{L} = \mathcal{L}_{eI} + \tfrac{1}{2} Q \left[\frac{\dot{s}}{s} \right]^2 - g k_B T_{\text{ext}} \ln(s) \ , \quad (4)$$

where $\mathcal{L}_{eI}$ is given by Eq. (1). s is the degree of freedom associated with the external reservoir in thermodynamical equilibrium with the $\mathcal{N}$ ions of the system; Q is a parameter of dimension energy times time squared, which plays the role of a *mass* for the motion of s. The second and third terms on the right-hand side of Eq. (4) are, respectively, the kinetic and potential energy for the variable s, where g is equal to the number of ionic degrees of freedom ($3\mathcal{N}$) and k_B is Boltzmann's constant. Since the ions only are coupled to the external system, the equations of motion for $\{\psi_i\}$ are the same as those derived from the Lagrangian (1); the equations of motion for $\{R_I\}$ and s are

$$M_i \frac{d}{dt}(s\dot{\mathbf{R}}_I) = -s\nabla_{\mathbf{R}_I} E \ , \tag{5}$$

$$Q\frac{d}{dt}\left[\frac{\dot{s}}{s}\right] = \sum_I M_I \dot{R}_I^2 - g k_B T_{\text{ext}} \ . \tag{6}$$

This computational scheme makes it possible to keep the average temperature of the ionic system constant during the MD runs. In addition, the electronic coordinates must be periodically quenched, in order to keep them near their proper BO states and thus accomplish a correct computation of time averages. We notice that, unlike other CT techniques proposed in the literature, the Nosé approach allows us to reproduce the canonical probability density in the phase space of the nuclei.[50]

B. Computational details

We have computed statistical averages for a-C within the microcanonical ensemble, e.g., by solving the coupled equations of motion (2) and (3); the calculation for l-C, which turned out to be a metallic system, has instead been performed within the canonical ensemble, e.g., by solving Eqs. (2), (5), and (6). We have carried out the MD simulations for 54 carbon atoms with periodic-boundary conditions, corresponding to a fcc supercell with macroscopic density ρ_d fixed to be 2 g cm^{-3}. The chosen density is appropriate for an amorphous form of C at low T (whereas glassy states have lower density), and, according to the (ρ_d, T) diagram of Ref. 24(a) and the results of Ref. 14, it is possibly a reliable density for the liquid as well, at low P. The electronic Kohn-Sham orbitals at the Γ point of the Brillouin zone (BZ) have been expanded in plane waves, with a cutoff (E_{cut}) of 32 Ry, implying the use of about 12 000 plane waves. At $\mathbf{k}=0$, one can choose the single-particle orbitals to be real, since the phase factor of the wave function is arbitrary. Thus, for each reciprocal lattice vector $\mathbf{G}$, the Fourier components $c(\mathbf{G})$ of the orbitals satisfy the symmetry relation: $c(-\mathbf{G})=c^*(\mathbf{G})$. In our computational procedure, we have explicitly taken advantage of this property, and used it to reduce the size of the basis set of a factor of 2.

The interaction between valence and core electrons has been described by the pseudopotential derived in Ref. 51 [Bachelet, Hamann, and Schlüter (BHS)], expressed in the form suggested by Kleinman and Bylander[52] (KB). The explicit form of the core-valence potential ($\hat{V}$) is

$$\hat{V} = \frac{|\Delta v_0 \phi_0\rangle\langle\phi_0 \Delta v_0|}{\langle\phi_0|\Delta v_0|\phi_0\rangle}\hat{P}_0 + v_1 \ . \tag{7}$$

$\hat{P}_0$ indicates a projection operator. $\psi_{0,0}=\phi_0 Y_{0,0}$ is the s eigenfunction of the atomic pseudoHamiltonian, in which the core-valence interaction has been replaced by the pseudopotentials[51] v_0 and v_1, for s and p states, respectively. Δv_0 is a short-ranged term given by the difference $(v_0 - v_1)$. Only the $l=0$ potential has been treated as nonlocal; potentials for $l \geq 2$ have been assumed to be equal to v_1. $\hat{V}$ is a fully nonlocal operator, since it acts in a different way on different angular *and* radial components of the wave function. The ground state of the carbon atom, s^2p^2, has been considered as reference configuration. The transferability of the KB pseudopotential to diverse atomic (e.g., sp^3) and ionic (e.g., s^2p and sp^2) configurations has been found to be as good as that of the BHS pseudopotential. No spurious solutions of the KB-pseudo-Hamiltonian (e.g., of the kind pointed out in Ref. 52) have been found for the carbon atom. The fully nonlocal form for $\hat{V}$ considerably improves the efficiency of the computational technique with respect to the use of a semilocal one, leading to a 35% reduction of the computer time needed for each MD step. Indeed, it allows plane-waves matrix elements to be written in a complete separable fashion, in Fourier space.

TABLE I. Equilibrium lattice constant (a_{eq}) of diamond, computed as a function of plane waves cutoff (E_{cut}), and number of **k** points used for BZ integrations (N_{k}). A fcc cell with two atoms has been used or this calculation. The experimental value for a_{eq} is 3.57 a.u.

N_k \ E_{cut} (Ry)	20	35	50	90
2	3.73	3.65	3.56	3.52
10	3.69	3.65	3.55	3.52

Several tests have been performed in order to establish the accuracy of the chosen basis set, pseudopotential, and cell size. In Table I, we report the computed values of the equilibrium lattice constant of diamond at $T=0$, as a function of E_{cut} and the number of **k** points (N_k). Table II displays the equilibrium bond length (R_{eq}) and vibrational frequency of C_2, obtained with different choices of E_{cut}. The trends observed, as well as the comparison of our results with those of other LDA computations and experiment, indicate that a cutoff of about 35 Ry gives a reliable description of the bonding properties of these systems. Analogous results have been found for the C_3 molecule. Our calculation with $E_{\text{cut}}=35$ Ry correctly predicts a linear ground-state geometry, and $R_{\text{eq}}=2.495$ a.u., to be compared with the value of 2.46 obtained in all-electron LDA computations.[41] Typical bond lengths are 3–4 % longer than fully converged results. For C_2, C_3, and diamond, we have also explicitly checked that the semilocal[51] and fully nonlocal[52] forms of the

TABLE II. Bond length ($\mathbf{R}_{\text{eq}}$) and vibrational frequency (ω) of the C_2 molecule, computed for the singlet $^1\Sigma$ state, as a function of plane waves cutoff (E_{cut}). A cubic cell with an edge of 16.0 a.u. has been used for these computations. The values for $\mathbf{R}_{\text{eq}}$ and ω obtained from local-density–all electron (LDA-AE) calculations are from Ref. 41(b). In our calculations we have not included spin efects, and therefore only the state $^1\Sigma$ has been considered here.

E_{cut} (Ry)	$\mathbf{R}_{\text{eq}}$ (a.u.)	ω (cm^{-1})
20.0	2.52	1467
27.5	2.47	1671
35.0	2.42	1779
LDA-AE	2.43	1750

pseudopotential give the same results for their bonding properties.

In order to test the accuracy in computing Fourier space sums with only the Γ point, we have calculated the total energy ($E_{\rm tot}$) of two-dimensional (2D) graphite as a function of N_k and of the number of atoms in the cell: $E_{\rm tot}$ has been computed in one case for a four-atoms orthorhombic cell, with 1, 4, 8, and 16 special points, and in the other case with Γ only, for 4, 8, 16 and 24 atoms cells. The comparison between the results obtained in the two cases is displayed in Fig. 1. This shows that a calculation for 3D graphite with a cell of 48 atoms and the Γ point is approximately as accurate as a computation for an elementary cell and 32 k points. It has been shown in Ref. 38(a) that a calculation with only 6 k points gives reliable structural properties of graphite (in-plane lattice constant, interlayer spacing, and isotropic bulk modulus in good agreement with experiment), and correctly predicts graphite to be more stable than diamond, when $E_{\rm cut}=35$ Ry is used. We note that for disordered systems the choice of the Γ point is a natural one, since $\mathbf{k}=\mathbf{0}$ is the sole high-symmetry point for their charge density.

The structural properties of a-C and l-C have been determined by occupying the lowest lying electronic states, without considering thermal broadening effects. This amounts to the neglect of fairly small corrections on most properties, since even for the highest T considered in our simulation (5000 K) $T/T_f \simeq \frac{1}{20}$, where T_f is the Fermi temperature. We have checked (see Sec. IV B) that even in the case of resistivity, which is mostly affected by the electronic states around the Fermi surface, the inclusion of thermal broadening does not affect qualitatively our results.

In the simulation runs a time step (Δt) equal to 4 a.u. for a-C and 3 a.u. for the high-T liquid has been used and the fictitious mass parameter μ set at 200 a.u. An optimal value of Q has been determined to be 1.2×10^5 a.u. In the simulation of a-C, the initial atomic positions have been chosen by randomly displacing the atoms from the positions in a perfect diamond lattice and the evolution in time followed for about $3000\Delta t$, using $E_{\rm cut}=20$ Ry. The configuration thus obtained has been heated up to 5000 K, evolved for another $3000\Delta t$, and finally cooled down to a rate of 10^{16} K/sec. After an equilibration of about $3000\Delta t$ at room temperature, a new annealing has been repeated with a higher cutoff, 32 Ry, and another a-C structure generated. The results obtained in the two cases are largely similar, the main difference being the overestimation of bond distances (about 6%) when using $E_{\rm cut}=20$ Ry. This is consistent with the results obtained for carbon molecules and diamond (see Tables I and II).

The liquid was obtained by heating up the final equilibrated a-C structure. As already mentioned, melting and the equilibration of the system at high T have been achieved with a CVT-MD technique. The temperature was raised of 300 K every 700 steps, corresponding to a heating rate of 10^{16} K/sec, up to 5000 K. Quenches of the electronic coordinates to their BO surface were performed every 400–500 MD steps; in general, 200–300 steepest descent steps were sufficient to minimize the total electronic energy. Statistical averages have been computed as time averages over about 10 000 steps, at $T=5000$ K. The average macroscopic temperature was constant within 1%. The results obtained from averaging over a shorter interval (6500 steps) have been found to be nearly identical, thus confirming that a reliable equilibration of the system had been achieved.

III. AMORPHOUS CARBON

A. Structure

We first describe the structure found for a-C, which was generated as described above, by quenching from a liquidlike (but not fully equilibrated liquid) state.

The structure of the computer-generated network at 300 K is found to be predominantly graphitic. It consists of 85% threefold and 15% fourfold coordinated atoms, where coordination is defined by our considering neighbor atoms to lie at distances less than the first minimum (r_m) of the particle-particle correlation function $g(r)$. This is shown in Fig. 2 by the dotted line. Threefold

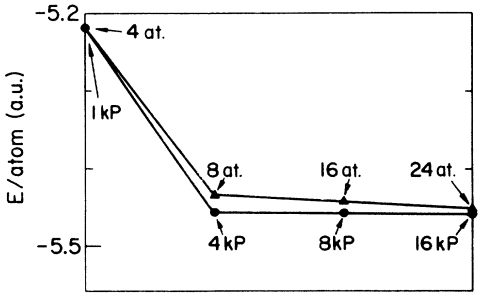

FIG. 1. Total energy per atom (E) of two-dimensional graphite computed as a function of number of $\mathbf{k}$ points used for BZ integrations ($N_{\rm k}$), and of the number of atoms (at.) included in the cell (see text). A plane-wave cutoff of 18 Ry has been used for this calculation.

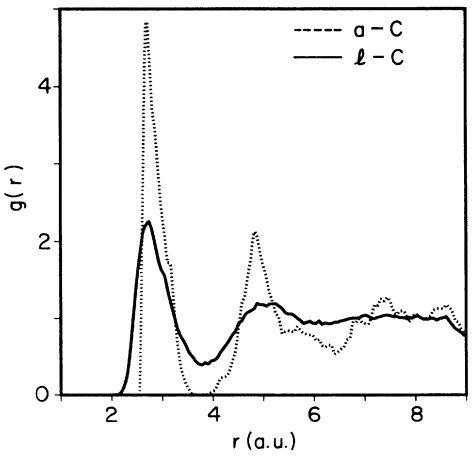

FIG. 2. Computed radial distribution functions $g(r)$ for a-C (dotted line) and l-C (solid line).

atoms can be regarded as nearly ideal sp^2 sites: Their nearest-neighbor distance, as computed from the first maximum of the partial correlation function[53] g_{33}, is equal to the calculated bond length in graphite at $T=0$, and their average bond angle is 117°, slightly smaller than that of graphite [see Fig. 3(a)]. On the other hand, fourfold atoms occur in distorted sp^3 structures. Indeed, the position of the first peak of g_{44} is at a distance 6% larger than the computed first-neighbor distance in diamond at $T=0$, and the angular distribution of sp^3 structures, shown in Fig. 3(a), has a peak at 105°.

RNM calculations[12] are consistent with ours, since the results for networks containing 91% sp^2 sites fit the experimental radial distribution functions (RDF's) better than those containing 50% or 100% sp^2 sites. Also the computer simulation with empirical potentials reported by Tersoff[14] yields a concentration of fourfold coordinated atoms (c_{sp^3}), 9%, in qualitative agreement with our findings.

Experimental estimates of c_{sp^3} ranging from 5 to 50% have been obtained from the analyses of RDF's,[5-9] derived from Fourier transforms of structure factors measured by x-ray scattering. The large proportion of sp^3 sites first proposed by Kakinoki *et al.*[7] (50%) has later been questioned,[5] since their imposition of an estimated macroscopic density to normalize the experimental data may not be strictly valid. An upperbound value of 12% for c_{sp^3} has been extrapolated from the sum rule on the complex dielectric function of *a*-C;[15] however, this procedure for the determination of the sp^2:sp^3 concentration does not appear to be completely reliable, according to the very recent investigation by Gao *et al.*[11(c)] The $(e,2e)$ data reported by these authors indicate that the sp^2 sites concentration (c_{sp^2}) is 0.85–1.0 in evaporated films, and 0.75–1.0 in ion-sputtered materials. These results are consistent with those of NEXAFS and EXAFS studies,[10] where c_{sp^2} of sputtered films is estimated to vary from 60% at $T=30$ °C, to 80% and 90% at $T=720$ and 1050 °C, respectively. This increasing graphitic character of *a*-C films, as the temperature is raised, has also been found in other experiments[4,7] and is confirmed by our computer simulation. Indeed, the number of sp^3 sites increases when the system is cooled down in our annealing procedure, while the twofold coordinated atoms present at $T \geq 2500-3000$ K disappear. Experimentally, an indication of the absence of significant *sp* component in *a*-C for $T \leq 1000$ °C comes, e.g., from the peak positions and width of the NEXAFS spectra reported in Ref. 10.

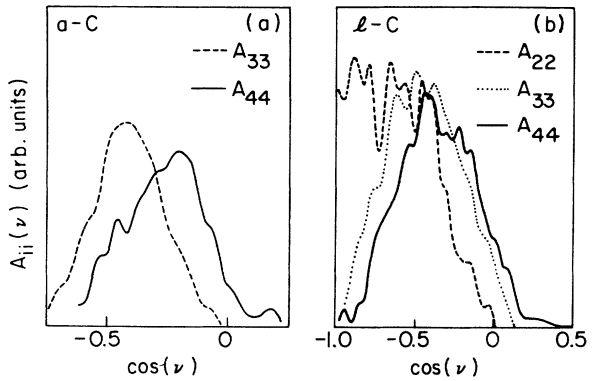

FIG. 3. Computed angular distributions $[A_{i,i}(\nu)]$ of (a) *a*-C and (b) *l*-C, for differently coordinated sites. $A_{2,2}$, $mA_{3,3}$, and $A_{4,4}$ are represented by the dashed, dotted, and solid line, respectively. ν indicates bond angles.

Our calculation reveals that sp^3 sites show a tendency to cluster. Indeed the ratio $\int^{r_m} dr\, g_{44} / \int^{r_m} dr\, g_{34} = 0.33$ is considerably larger than the value $N_4/N_3 = 0.17$, which one would obtain for randomly distributed fourfold coordinated atoms (N_3 and N_4 indicate the number of sp^2 and sp^3 sites, respectively). The clustering of sp^3 sites may be important in understanding both electronic and hardness properties of *a*-C films.

In Table III we report the calculated positions of the first and second peak of the RDF $J(r)$ [$J(r)=4\pi\rho_d r^2 g(r)$] and the first-shell coordination number, together with the corresponding quantities obtained from different measurements. In addition to the good agreement with experiment for the features listed in the table, the overall characteristics of $J(r)$ are nicely reproduced in our computer simulation. This can be seen from Fig. 4, where we compare the computed $J(r)$ with the one obtained from electron diffraction (ED) by Kakinoki *et al.*[7] RDF's derived in different ED experiments have similar characteristics; the one we have chosen here is perhaps the most accurate, i.e., obtained from measurements performed with the largest cutoff wave vector (27 Å^{-1}). The theoretical $J(r)$ has been convoluted with the experimental resolution function, but has not been scaled for different theoretical and experimental densities, due to large uncertainties on the latter.[5] We note that the convolution affects not only the width of the peaks but their position as well: A convolution function appropriate to the cutoff wavelength adopted in Ref. 8 (8.8 Å^{-1}), for example, gives a first-neighbor distance larger than

TABLE III. Positions of the first (r_1) and second (r_2) peak of the radial distribution function $J(r)$ of *a*-C, and first (n_1) shell coordination number, as obtained from different experiments and from theory. ρ_d is the macroscopic density of the system. Theoretical results corresponding to both the unconvoluted (*) and convoluted (†)$J(r)$ (see text) are shown.

Noncrystalline C	r_1 (Å)	n_1	r_2 (Å)	ρ_d (g cm^{-3})
Glassy carbon[a]	1.42	2.99	2.45	1.49
Evaporated *a*-C[b]	1.50	3.45	2.53	2.40
Evaporated *a*-C[c]	1.43	3.30	2.53	2.10
a-C from PTFE[d]	1.46		2.54	
Plasma deposited *a*-C[e]	1.44		2.54	
a-C (theory)[f]	1.44*	3.20	2.56*	2.00
	(1.48†)	3.20	(2.64†)	

[a]Reference 5.
[b]Reference 7.
[c]Reference 8.
[d]Reference 9. [*a*-C films prepared by reduction of polytetrafluoroethylene (PTFE) with alkali-metal amalgams.]
[e]Reference 10.
[f]Present work.

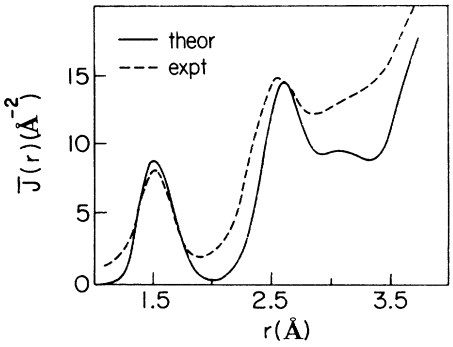

FIG. 4. Theoretical (solid line) and experimental (dotted line; Ref. 7) radial distribution functions $J(r)$ of a-C.

that of Fig. 4 by 4%. It has been argued[5] that the presence of threefold and fourfold coordinated atoms in a-C should be revealed by the existence of a double first peak in the particle-particle correlation function. We instead find that the first maximum of $g(r)$ is unique but the presence of sp^3 sites is revealed by a very weak shoulder, which could be detected only by experiments using extremely high wavelength cutoff ($q \geq 70$ Å^{-1}).

From our calculation we can determine individual atomic positions of our system, from which a detailed picture of the network can be extracted. Although the computer generated a-C is a truly three-dimensional structure, the atoms may be viewed as arranged into several "thick planes": Two labeled a and b in Fig. 5(a), are roughly parallel to each other, with a stacking sequence reminiscent of that of graphite (a,b,a). They are connected by orthogonal planes [indicated by c and d in Fig. 5(a)], whose distance is much smaller than that between graphite planes. Although most of the bonds formed by sp^2 atoms tend to lie nearly on the same plane, as in graphite, substantial buckling can occur locally, giving these planes a finite thickness of about 1.0–1.2 a.u.

A ring statistic analysis shows that a-C is mainly composed of fivefold, sixfold, and sevenfold rings, with several coupled (5+7) ones similar to those found in carbon azulene molecules [see Fig. 5(b)]. The presence of pentagonal rings in sputtered carbon films has been first proposed by Nelson,[16(a)] based on the energetics of carbon bonds in the film surface, during growth. Other indications of the presence of odd-membered rings in a-C, and, in particular, of C_5 and C_7 units, come from the electron diffraction study of Weissmantel *et al.*[16(b)] and the EXAFS measurements reported by Comelli *et al.*[10] Very recently, scanning tunneling microscopy (STM) has been used to unravel the structure of a-C surfaces:[16(a)] Several patterns consisting of interconnected sixfold- and fivefold-membered units have been observed, consistent with our findings [see Fig. 5(b)].

B. Electronic properties

Figure 6(c) displays the computed electronic density of states (EDOS) together with the peak positions of the ultraviolet photoemission spectra (UPS) and x-ray-absorption near-edge structure spectra (XANES) report-

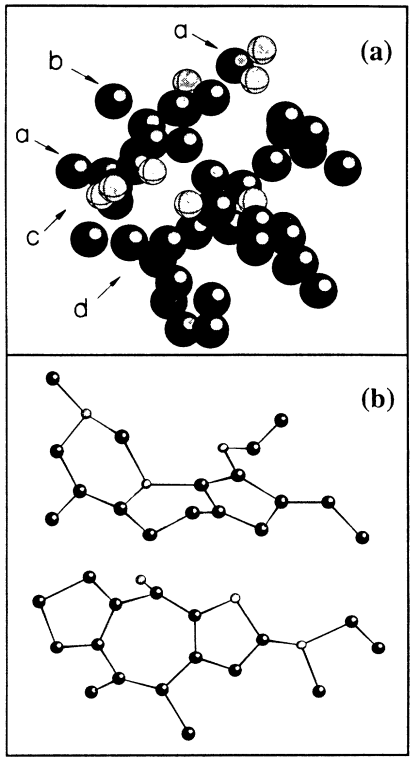

FIG. 5. Microscopic structure of the computer-generated a-C network: (a) the entire set of atoms belonging to one MD cell and (b) several fivefold, sixfold, and sevenfold ring structures the system is composed of are displayed (see text). Black and grey spheres indicate threefold and fourfold coordinate atoms, respectively.

ed in Refs. 15(a) and 15(b), respectively. The description of the electronic states, which are the result of the same self-consistent procedure from which the atomic positions were derived, is in good agreement with experiment. In the valence band, the split s peak around -16 eV and the broad σ peak centered at about 7 eV are correctly reproduced, as well as the π state shoulder near the Fermi level (E_F), present in graphite and a-C but, of course, not in diamond [see Figs. 6(a) and 6(b)]. The conduction-band spectrum shows a sharp π^* peak and a broader σ^* peak, in agreement with experimental findings. A comparison of our results with the measured intensities for the various peaks appears to be quite difficult. Indeed, the effect of cross-section (σ_c) modulation in the photoemission intensity for the valence band of carbon has been found to be particularly large,[15(b)] due to the large ratio $\sigma_c(2s)/\sigma_c(2p)$ deriving from the different nodal properties of the $2s$ and $2p$ wave functions. Furthermore, a different relative intensity of the π^* and σ^* peaks in the conduction band is reported in different experiments[15(b)] (XANES and Auger-ANES), to indicate strong effects from both core-hole interaction and matrix elements.

As shown in Fig. 6(c), we find a deep minimum in the EDOS of a-C, near E_F. Within the finite resolution of our calculation, this is consistent with the experimental observation[4] of a small gap of about 0.4–0.4 eV. Tight-

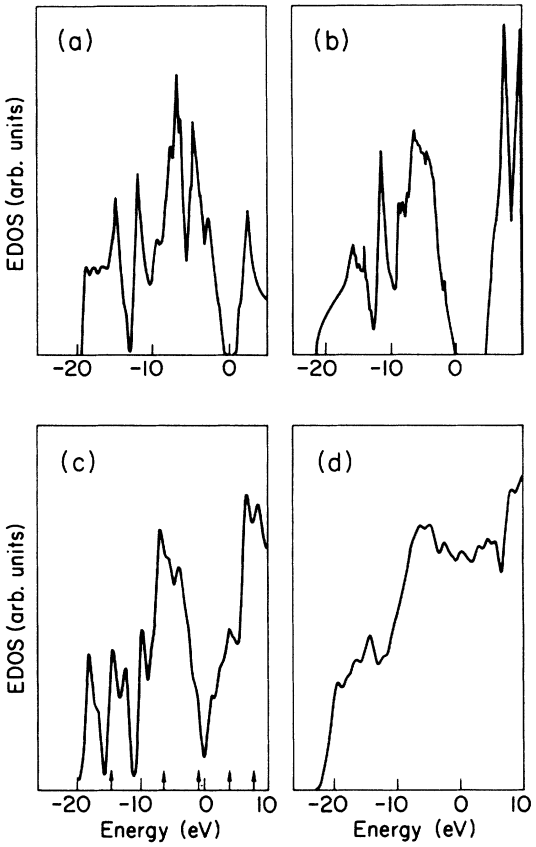

FIG. 6. EDOS of (a) rhombohedral graphite, (b) diamond, (c) a-C, and (d) l-C, as computed within LDA. The zero of the energy scale corresponds to the Fermi energy. The results displayed in (a) and (b) are from Ref. 38(b) whereas those in (c) and (d) have been obtained in the present work. In (c) the arrows indicate positions of experimental peaks (Ref. 15).

binding (TB) models[13] developed for the networks proposed in Ref. 12 show instead metallic features in the EDOS of all the structures containing sp^2 sites. In order to understand this discrepancy (that is, if due to assumptions on the atomic structure or to inadequacies of the TB picture), we have computed the EDOS for the network generated in our *ab initio* simulation with a TB Hamiltonian.[54] An sp^3 basis set in which π_z and (π_x,π_y) orbitals are treated equivalently has been adopted, and only first-neighbor interactions included. In the TB model by O'Reilly and Robertson,[13] π_x-π_y interactions have instead been treated differently from those involving π_z electrons. This is probably motivated by their RNM structures, which are composed of warped graphite layers with a preferred z direction.[12] Interaction parameters have been taken from Chadi's model for carbon,[54] and their scaling law chosen to be d^{-2} for all first-neighbor distances d. Our results show a metallic behavior for a-C, the ratio between EDOS at the valence-band peak and at E_F being very similar to that found in previous models.[4(a),13]. This seems to indicate difficulties of applying the TB picture to a-C; i.e., lack of transferability of TB parameters between differently coordinated bonded forms of carbon, and/or inadequacy in a simple scaling law such as that chosen here. We note that the d^{-2} scaling is expected to be valid for bond lengths close to those of graphite and diamond, e.g., for the characteristic distances of the structures whose properties have been fitted in the derivation of the TB interactions. The minimum of a-C $g(r)$, used as first-neighbor cutoff in our model, is instead much larger (about 30%). Furthermore, the pp-π interactions between π and σ orbitals have been shown to be strongly structure dependent also for diamond and graphite.[55]

IV. LIQUID CARBON

Our simulation for l-C has been performed at the same fixed density ($\rho_d = 2$ g cm^{-3}) as that considered for the amorphous material. According to the (ρ_d, T) diagram of Ref. 24(a), this is possibly a reliable density for the liquid at $T = 5000$ K. Furthermore, the results of the simulation with empirical potential by Tersoff,[14] indicate a liquid density of about $\rho_d = 1.8$ g cm^{-3} in the low-P regime. *A posteriori* we can calculate the pressure of the liquid state that has been generated: the value which we have estimated suggests that our investigation of l-C properties is relevant to low-P experiments.

A. Structure

As we already mentioned, the liquid was obtained by heating up the a-C structure generated at room temperature. The main transformation as the temperature is raised concerns the appearance of twofold coordinated atoms at $T = 2500$–3000 K (their concentration increasing almost continuously with increasing T up to 5000 K), accompanied by the onset of metallic features, as a result of π and π^* states meging. At temperatures around 4000 K, the system begins showing a diffusive behavior, possibly to indicate that a melting transition is taking place. Above 4500 K, the continuous increase of the atomic mean-square displacement as a function of simulation time shows that a liquid state has been generated. Temporal averages to compute electronic and atomic properties have been taken at $T = 5000$ K: At this temperature the self-diffusion coefficient of the system is calculated to be 2.4×10^{-4} cm^2 sec^{-1}.

The structural modifications observed at $T = 2500$–3000 K are consistent with the model proposed by Heinman *et al.*,[44(b)] in which high-T treatment of graphite is supposed to lead to carbon polytypes with sp configuration and carbon-carbon chains. This model supports the hypothesis that graphite is not stable at high T, but transforms to the carbyne allotrope of carbon. However, several authors have questioned the existence of a carbyne region in the C-phase diagram.[49] In particular, it has been pointed out that the diffraction patterns and the results of spectroscopic measurements which seem to indicate structural transformations in high-T graphite may have been misinterpreted, in that they may not belong to pure carbon but to sheet silicates.

In our calculation, we find that the liquid state as 5000 K is composed of 32% twofold, 52% threefold, and the

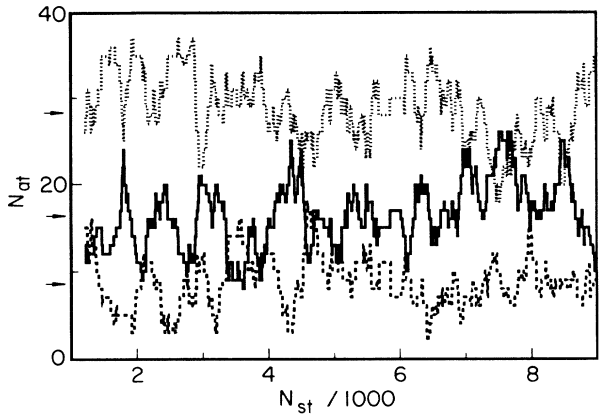

FIG. 7. The number of twofold (solid line), threefold (dotted line) and fourfold (dashed line) coordinated atoms (N_{at}) present in the liquid state at $T=5000$ K, as a function of simulation time. N_{st} indicates the number of MD steps. Arrows indicate the average number of differently coordinated sites.

remaining fourfold coordinated atoms. Atomic coordination as a function of simulation time is shown in Fig. 7. This shows (i) the constantly changing coordination of each site and (ii) that our simulation time is long enough to compute meaningful averages. Unlike what has been found for silicon,[34(a),34(b)] the average coordination of the system decreases upon melting; we calculate it to be 2.9 in the liquid, against the value of 3.2 computed for a-C. As indicated by the peak positions of the radial distribution functions $g(r)$, shown in Fig. 1 for both l-C and a-C, the average first-neighbor distance slightly decreases in the liquid, whereas the second-neighbor distance becomes larger. This behavior is again opposite to that observed in the amorphous to liquid transition in silicon.

A description of the differently coordinated sites present in l-C is provided by the analysis of the partial correlation functions[53] $g_{ii}(r)$, and $g_{ij}(r)$, displayed in Fig. 8, and of the angular distributions A_{it} $[i,j=2,3,4]$, shown in Fig. 3(b). Fourfold coordinated atoms, found to be distorted sp^3 structures in a-C, appear to have different bonding properties in the liquid. Indeed, g_{44} and A_{44} indicate that these sites have a wide range of preferred bond lengths, spread over an interval of about 1 a.u., as well as of bond angles, ranging from 90° to 115°. In particular, each of these atoms are found to have four bonds of different length, quite unlike an sp^3 diamond site. The threefold coordinated atoms may be viewed as distorted graphitic sp^2 units: The first maximum of g_{33} is at a distance slightly larger (4%) than the computed bond length for graphite at $T=0$, and the peak of A_{33} lies between 110° and 125°. When linked to each other, the average bond distance of twofold sites is 2.55 a.u., a few percent larger than the bond lengths obtained for C_2 (2.430 a.u.) and C_3 (2.495 a.u.) molecules. This suggests that these atoms are mostly triple bonded, according to the classification of carbon bonds given, e.g., by Coulson.[56] The angular distribution A_{22} shows that angles between 180° and 110° are almost equiprobable, whereas those smaller than 100° are very unlikely. This is consistent with the geometries of C_3 and C_4 molecules detected in C vapors: They have a linear structure, but very small bending frequencies.[41] The ratio $(\int dr\, g_{23}/\int dr\, g_{24})=3.0$ (where the integrals are extended from zero up to r_m) indicates that twofold sites are preferably connected to threefold rather than fourfold ones, and the peak of g_{23}, between 2.55 and 2.80 a.u., suggests a possible alternation of sp-sp^2 bonds, differing in their proporation of π character. A bond alternation of the kind —C=C— has been proposed, for example, for the ground state of infinite carbon chains.[57] We finally notice that the second peak of $g(r)$ arises mainly from the second-neighbor distribution of threefold coordinated atoms.

From a ring statistic analysis we find that N-fold rings with N larger than 9, i.e., chainlike structures, are the great majority in the liquid, although fivefold, sixfold, and sevenfold membered units are also present; in contrast, the low T (300 K) a-C was found to have essentially no rings with N larger than seven. A "snapshot" of the system, showing its differently coordinated sites and characteristic rings, is displayed in Fig. 9; in this picture we have plotted several atoms of a representative instantaneous configuration, chosen so that the atomic coordination be close to the average one.

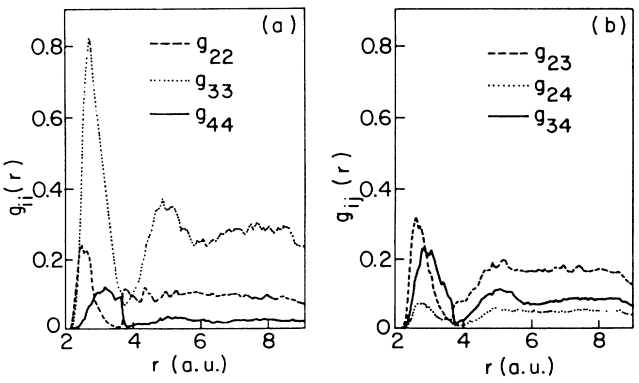

FIG. 8. Radial distribution functions (a) $g_{i,i}$ and (b) $g_{i,j}$ $(i\neq j)$ of l-C, $i,j=2,3,4$.

B. Electronic properties

Figures 6(d) and 10 show the computed electronic EDOS and electrical conductivity (σ) of l-C, respectively. These have been obtained as averages over ten atomic configurations, chosen among the total number generated in our computer simulation, one about every 1000 steps. The accuracy of the calculation has been checked by computing the density of occupied states using all 10 000 configurations, which turns out to be nearly identical to that displayed in the picture.

Our results show that the liquid at low pressure is a metal. The electronic properties of l-C have been greatly debated in the literature. Bundy[18] has shown that l-C is metallic in the pressure regime $10\leq P\leq 110$ kbar, whereas an earlier investigation suggested that molten graphite is insulating in the pressure range of 120 to

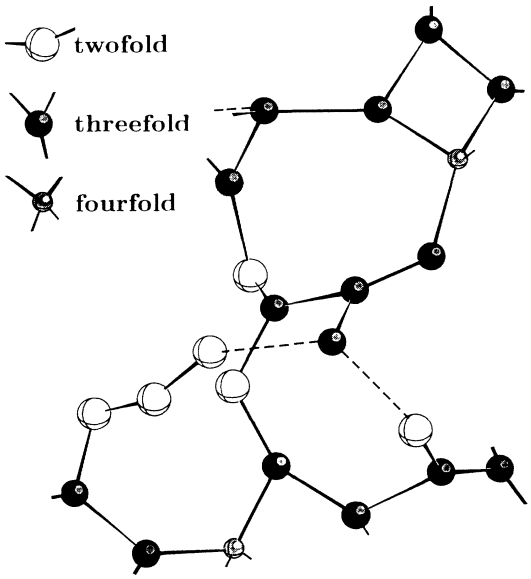

FIG. 9. Several atoms of a representative configuration of *l*-C are displayed (see text). White, black, and grey spheres indicate twofold, threefold, and fourfold coordinated atoms, respectively. Bonds with length close to the first minimum of the correlation function $g(r)$ (see Fig. 2) have been represented as dotted lines.

several hundred bars.[28] More recently, Malvezzi *et al.*[20(a)] have reported time-resolved optical measurements of laser-excited graphite, where the reflectivity of the high-temperature phase, assumed to be a liquid, is found to be lower than that of the starting material. This would indicate that *l*-C is a semi-insulator. These results are consistent with the resistivity studies by Chauchard *et al.*[20(b)]—who observed a large decrease of graphite samples resistivity under laser illumination—but in disagreement with optical and dc conductivity measurements reported by Heremans *et al.*[21(a)] Indeed, these authors find an increase in the reflectivity, as well as resistivity, of highly oriented pyrolitic graphite upon melting, and they measure a nearly temperature independent resistivity for the liquid phase, whose low value ($\rho_r = 30-70$ $\mu\Omega$ cm) is certainly characteristic of a metal. A discussion of the possible diferences in the experimental results of Refs. 20 and 21 is given in Refs. 21 and 23. Melting of graphite and diamond in anvil apparatus, at pressures ranging from 2.5 to 18 kbar, has been reported very recently by Togaya.[22] The melt formed in both cases is found to be metallic or semimetallic, with a resistivity estimated to be lower than 400 $\mu\Omega$ cm. We finally note that in the femtosecond laser melting of graphite of Reitze *et al.*,[23] graphite is found to exhibit metallic optical properties (i.e., sharply increased reflectivity) for several picoseconds after excitation above the critical melting fluence, but then to develop insulating properties (i.e., reduced reflectivity). These results might indicate that the equilibrium state of the liquid is nonmetallic, or that *l*-C can form in either insulating or conducting form, depending on excitation conditions.[23]

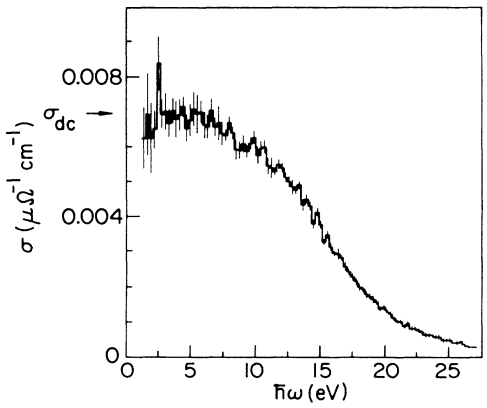

FIG. 10. Electrical conductivity (σ) of *l*-C, computed as average over ten atomic configurations (see text). The extrapolated conductivity at zero [$\sigma(\omega \to 0)$] gives a dc value of about 0.007 $\mu\Omega\,\mathrm{cm}^{-1}$.

In our calculation, the electrical conductivity as a function of frequency (ω) has been obtained from the Kubo-Greenwood formula[58]

$$\sigma = \frac{2\pi\hbar^2 e^2}{3m^2 V\omega} \sum_{i,i'} (f_{i'} - f_i) |M_{i,i'}|^2 \delta(\varepsilon_{i'} - \varepsilon_i - \hbar\omega) , \quad (8)$$

where $|M_{i,i'}|$ is the momentum operator matrix element between states i' and i whose occupation numbers, $f_{i'}$ and f_i, are treated as Fermi-Dirac distributions. It is essential to carry out such a calculation to make definite conclusions about the conductivity of *l*-C. Indeed, localization effects due to disorder are properly accounted for in Eq. (8), which can therefore distinguish between metallic and insulating properties in disordered systems. We find that in the range $\hbar\omega \leq 12-13$ eV, σ can be approximated by a Drude-like function, whereas its fall off at higher frequencies is much more rapid: This feature is at least partially an artifact, due to the finite range of energies considered in our calculation. From the limit of Eq. (8) for $\omega \to 0$, an estimate of the dc electrical conductivity (σ_{dc}) and of the resistivity ($\rho_r = 1/\sigma_{dc}$) of the system can be extracted. The main contribution to σ_{dc} comes from electrons with energies close to the Fermi level (E_F). Indeed, the results obtained from Eq. (8) and from the approximate expression[59]

$$\sigma_{dc} = \frac{2\pi\hbar^3 e^2}{m^2} a [N(E_F)]^2 , \quad (9)$$

a being the average nearest-neighbor distance, agree within 10%. The computed value of ρ_r is 140 ± 28 $\mu\Omega$ cm; this is compared with the available experimental results in Table IV. We note that uncertainties upon the calculated resistivity are introduced by finite-size effects and inaccuracies can possibly derive from the LD approximation of density-functional theory. The comparison with experiment shown in the table can only be qualitative: Indeed, the macroscopic density of the liquid obtained experimentally is not known, neither is the volume change that carbon undergoes upon melt-

TABLE IV. Electrical resistivity (ρ_r) of l-C, and corresponding pressure (P) of the system, as obtained from different experiments and from theory. The theoretical results have been obtained by treating the occupation numbers f_i entering Eq. (8) (see text) as Fermi-Dirac distributions. If we consider the f_i the electrons would have at $T=0$, the computed value for ρ_r turns out to be 100 ± 20 $\mu\Omega$ cm.

	ρ_r ($\mu\Omega$ cm)	P (kbar)
Bundy[a]	150	≥ 10
Shaner[b]	1000	4
Heremans *et al.*[c]	30-70	$\simeq 0$
Togaya[d]	≤ 400	2.5–18
Theory[e]	140 ± 28	

[a]Reference 18.
[b]Reference 27.
[c]Reference 21.
[d]Reference 23.
[e]Present work.

ing. For example, Heremans *et al.*[21] assumed no volume changes as graphite fibers are melted, whereas Shaner[27] reported a 100% expansion of highly disordered graphite, upon melting. Furthermore, the comparison between the data displayed in Table IV suggests that the resistivity of l-C might be significantly dependent upon pressure.

V. SUMMARY AND CONCLUSIONS

We have presented detailed analyses of the structural and electronic properties of amorphous carbon at room temperature,[30(a)] and liquid carbon at low pressure,[30(b)] which we have investigated with a first-principles molecular-dynamics method.[31] The simulation of a-C has been carried out within the microcanonical ensemble. The liquid has been studied with a CVT technique: This approach has been found to be particularly appropriate to overcome the problem of energy transfer between electronic and ionic degrees of freedom, which may occur in the simulation of metallic systems with the original method of Refs. 31 and 32.

In our calculation, we find a-C to be predominantly graphitic, with a concentration of sp^3-diamondlike sites of about 15%, in agreement with most experiments and, in particular, with very recent $(e,2e)$ spectroscopy[11] and EXAFS (Ref. 10) studies. A new feature revealed by our computer simulation regards the tendency of fourfold coordinated atoms to cluster: This may be relevant to the understanding of both electronic and hardness properties of a-C films. The network that we have generated results to be a three-dimensional structure, with the atoms arranged into *thick planes,* as shown in Fig. 5, and composed of even- and odd-membered rings, consistently with the findings of EXAFS (Ref. 10) and STM[16(a)] investigations. In our description of the electronic properties of a-C, we find that the peak positions of the computed EDOS are in good agreement with those of UPS[15(a)] and XANES[15(b)] spectra. Furthermore, the deep minimum of the density of states close to the Fermi energy is consistent with the experimental observation of a small gap for a-C films. However, the finite resolution of our calculation does not allow us to establish whether the system is a small-gap semiconductor or a semimetal.

The liquid state has been obtained by heating up the a-C structure generated at room temperature. The main transformation which we observe, as the temperature is raised, is the appearance of twofold coordinated atoms at $T=2500-3000$ K, accompanied by the onset of metallic features. At $T=5000$ K and low pressure, l-C is found to have an average coordination less than 3.0 and to be composed of differently coordinated atoms (twofold, threefold, and fourfold), which display a variety of bonds, from single to triple. These are mainly arranged into chainlike structures: Indeed, N-fold rings with $N\geq 9$ are the great majority in the system, although fivefold, sixfold, and sevenfold membered rings are also present. From the calculated electronic density of states and optical conductivity, we determine the liquid to be a good metal: This is in agreement with very recent reflectivity and resistivity experiments on laser-excited graphite,[21] and with resistivity measurements of diamond and graphite molten in anvil apparatus.[22] On the other hand, it is in apparent disagreement with the conclusions of earlier reflectivity studies,[20] and with the results of femtosecond time-resolved measurements of melting dynamics of graphite.[23]

In order to resolve these controversies and fully understand the nature of the liquid state, the dependence of its properties upon pressure and temperature should be investigated. Since the stable form of carbon at low T changes greatly, from graphite to diamond, with pressure, the nature of the liquid may be expected to change as well, as a function of P.[60] Although it has long been believed that the liquid is more dense than the solid, as it is the case for the other group-IV elements, recent experiments[1,3,29] indicate that the diamond-liquid phase boundary has a positive slope and therefore that the liquid is less dense than diamond. This may have relevant implications for the understanding of carbon phases in the earth mantle[3] and in outer planets.[2] These issues have been investigated by carrying our first-principles studies of liquid carbon and the melting of diamond at high pressures; our results are planned to be discussed in a separate report.[60]

ACKNOWLEDGMENTS

This work has been supported by the NSF Grant No. DMR86-12860 (G.G. and R.M.M.) and the Scuola Internazionale Superiore di Studi Avanzati—Centro Interuniversitario Nord-Est per il Calcolo Automatico CINECA collaborative project, under the sponsorship of the Italian Ministry for Public Education (R.C. and M.P.). Part of the computational work has been done at the National Center for Supercomputing Applications. We benefitted from useful discussions with D. J. Chadi, R. Grover, M. Grunbach, J. W. Shaner, J. Tersoff, and M. Togaya.

*Present address: IBM Research Division, Forschungslaboratorium Zurich, CH-8803 Ruschlikon, Switzerland.

[1]F. P. Bundy, Physica A **156**, 169 (1989), and references therein.

[2]M. Ross, Nature **292**, 435 (1981).

[3](a) J. S. Dickey, W. A. Bassett, J. M. Bird, and M. S. Weathers, Geology **11**, 219 (1983); (b) M. S. Weathers and W. A. Bassett, Phys. Chem. Minerals **15**, 105 (1987); (c) D. A. Young and R. Groover, in *Shock Waves in Condensed Matter* (Elsevier, New York, 1988), p. 131.

[4](a) J. Robertson, Adv. Phys. **35**, 317 (1986), and references therein; (b) K. Shimakawa and K. Miyake, Phys. Rev. Lett. **61**, 994 (1988).

[5]D. F. R. Mildner and J. M. Carpenter, J. Non-Cryst. Solids **47**, 391 (1982).

[6]D. R. Mckenzie, L. C. Botten, and R. C. McPhedran, Phys. Rev. Lett. **51**, 280 (1983).

[7]J. Kakinoki, K. Katada, T. Hanawa, and T. Ino, Acta Crystallogr. **13**, 171 (1960); **13**, 448 (1960); **18**, 578 (1965).

[8]B. T. Boiko, L. S. Palatnik and A. S. Derevyanchenko, Dokl. Akad. Nauk SSSR **179**, 316 (1968) [Sov. Phys.—Dokl. **13**, 237 (1968)].

[9]L. Cervinka, F. P. Dousek, and J. Jansta, Philos. Mag. B **51**, 604 (1985).

[10]G. Comelli, J. Stohr, C. J. Robinson, and W. Jark, Phys. Rev. B **38**, 7511 (1988).

[11](a) A. L. Ritter, J. R. Dennison, and R. Jones, Phys. Rev. Lett. **53**, 2054 (1984); (b) Y. Y. Wang, A. L. Ritter, T. J. Fabish, and J. A. Nemetz, Bull. Amer. Phys. Soc. **33**, 354 (1988); (c) C. Gao, Y. Y. Wang, A. L. Ritter, and J. R. Dennison, Phys. Rev. Lett. **62**, 945 (1989).

[12]D. Beeman, J. Silverman, R. Lynds, and M. R. Anderson, Phys. Rev. B **30**, 870 (1984).

[13]J. Robertson and E. P. O'Reilly, Phys. Rev. B **35**, 2946 (1987).

[14]J. Tersoff, Phys. Rev. Lett. **61**, 2879 (1989).

[15](a) J. Fink, T. Muller-Heinzer-ling, J. Pfluger, B. Scheerer, B. Dischler, P. Koidl, A. Bubenzer, and R. E. Sah, Phys. Rev. B **30**, 4713 (1984), and reference therein; (b) D. Wesner, S. Krummacher, R. Carr, T. K. Sham, M. Strongin, W. Eberhardt, S. L. Weng, G. Williams, M. Howells, F. Kampas, S. Heald, and F. W. Smith, Phys. Rev. B **28**, 2152 (1983).

[16](a) B. Marchon, M. Salmeron, and W. Sickhaus, Phys. Rev. B **39**, 12 907 (1989); (b) C. Weissmantel *et al.*, J. Vac. Sci. Technol. A **4**, 2892 (1979).

[17]J. C. Angus and C. C. Hayman, Science **241**, 913 (1988).

[18](a) F. P. Bundy, J. Chem. Phys. **38**, 631 (1963); (b) J. Geophys. Res. **85**, 6930 (1980).

[19]T. Venkatesan, D. C. Jacobson, J. M. Gibson, B. S. Elman, G. Braunstein, M. S. Dresselhaus, and G. Dresselhaus, Phys. Rev. Lett. **53**, 360 (1984).

[20](a) A. M. Malvezzi, N. Bloenbergen and C. Y. Huang, Phys. Rev. Lett. **57**, 146 (1986); (b) E. A. Chauchard, C. E. Lee, and C. Y. Huang, Appl. Phys. Lett. **50**, 812 (1987).

[21](a) J. Heremans, C. H. Olk, G. L. Eeseley, J. Steinbeck, and G. Dresselhaus, Phys. Rev. Lett. **60**, 453 (1988), and references therein; (b) J. Steinbeck, G. Braunstein, M. S. Dresselhaus, T. Venkatesan, and D. C. Jacobson, J. Appl. Phys. **58**, 4374 (1985).

[22]M. Togaya (unpublished).

[23]D. H. Reitze, X. Wang, H. Ahn, and M. C. Downer, Phys. Rev. B **40**, 11 986 (1990).

[24](a) H. R. Leider, O. H. Krikorian, and D. A. Young, Carbon **11**, 555 (1973); (b) D. M. Haaland, *ibid.* **14**, 357 (1976).

[25]R. Clarke and C. Uher, Adv. Phys. **33**, 469 (1984); I. A. Korsunskaya, D. S. Kamenetskaya, and I. L. Aptekar, Phys. Metals Metallogr. **34**, 39 (1972).

[26]A. Ferraz and N. H. March, Phys. Chem. Liq. **8**, 289 (1979).

[27]J. W. Shaner, Bull. Am. Phys. Soc. **32**, 607 (1987).

[28]M. T. Jones, National Carbon Research Laboratory, Report No. PRC3, 1958 (unpublished).

[29]J. W. Shaner, J. M. Brown, C. A. Swenson, and R. G. McQueen, J. Phys. (Paris) Colloq. **44**, C8-235 (1984); A. C. Mitchell, J. W. Shaner, and R. N. Keller, Physica **139**, 386 (1986).

[30](a) G. Galli, R. M. Martin, R. Car, and M. Parrinello, Phys. Rev. Lett. **62**, 555 (1989); (b) *ibid.* **63**, 988 (1989); (c) in *Proceedings of the Conference on Atomistic Modeling: Beyond Pair Potentials* (Plenum, New York, 1989), pp. 159–165.

[31]R. Car and M. Parrinello, Phys. Rev. Lett. **55**, 2471 (1985).

[32]R. Car and M. Parrinello, in *Simple Molecular Systems at Very High Density*, P. Loubeyre and N. Boccara, Vol. 186 of *NATO Advanced Study Institute Series B: Physics*, edited by A. Polian (Plenum, New York, 1988), p. 455.

[33]F. Buda, R. Car, and M. Parrinello, Phys. Rev. B **41**, 1680 (1990). F. Buda, G. L. Chiarotti, R. Car, and M. Parrinello, Phys. Rev. Lett. **63**, 294 1989; D. Allan and M. Teter, *ibid.* **59**, 1136 (1987).

[34](a) R. Car and M. Parrinello, Phys. Rev. Lett. **60**, 204 (1988); (b) I. Stich, R. Car, and M. Parrinello, **63**, 2240 (1989); (c) X. P. Li, P. B. Allen, R. Car, M. Parrinello, and J. Q. Broughton, Phys. Rev. B **41**, 3260 (1990); (d) G. X. Qian, M. Weinert, G. W. Fernando, and J. W. Davenport, Phys. Rev. Lett. **64**, 1146 (1980); (e) G. Galli and M. Parrinello, J. Phys. C (to be published).

[35]P. Ballone, W. Andreoni, R. Car, and M. Parrinello, Phys. Rev. Lett. **60**, 271 (1988); Europhys. Lett. **8**, 73 (1989); D. Hohl, R. O. Jones, R. Car, and M. Parrinello, Chem. Phys. Lett. **139**, 540 (1987), J. Chem. Phys. **89**, 6823 (1988); J. Am. Chem. Soc. **111**, 826 (1989); R. O. Jones and D. Hohl, J. Am. Chem. Soc. **112**, 2590 (1990); P. Ballone and G. Galli, Phys. Rev. B **40**, 8563 (1989); *ibid.* (to be published).

[36]W. Kohn and L. Sham, Phys. Rev. **140**, A1133 (1965).

[37]M. T. Yin and M. L. Cohen, Phys. Rev. B **24**, 6121 (1981); J. R. Chelikowsky and S. Louie, *ibid.* **29**, 3470 (1984); M. R. Salehpour and S. Satpathy (unpublished).

[38](a) M. T. Yin and M. L. Cohen, Phys. Rev. B **29**, 6996 (1984); (b) S. Fahy, S. Louie, and M. L. Cohen, *ibid.* **34**, 1191 (1986), and references therein; (c) M. Posternak, A. Baldereschi, A. J. Freeman, E. Wimmer, and M. Weinert, Phys. Rev. Lett. **50**, 761 (1983), and references therein.

[39]R. Biswas, R. M. Martin, R. J. Needs, and O. H. Nielsen, Phys. Rev. B **30**, 3210 (1984); **35**, 9559 (1987).

[40]M. T. Yin and M. L. Cohen, Phys. Rev. Lett. **50**, 2006 (1983).

[41](a) J. R. Chelikowsky and M. Y. Chou, Phys. Rev. B **37**, 6504 (1988), and references therein; (b) G. S. Painter and F. W. Averill, *ibid.* **26**, 1781 (1982).

[42]J. R. Heath *et al.* Comments Condens. Matter Phys. **13**, 119 (1987).

[43]J. D. Johnson, Bull. Am. Phys. Soc. **34**, 7, 1700 (1989).

[44]See, e.g., A. R. Ubbelohde, *The Molten State of Matter* (Wiley, New York, 1978).

[45]E. Kaxiras and K. C. Pandey, Phys. Rev. Lett. **61**, 2963 (1988).

[46]J. Bernholc *et al.*, Phys. Rev. Lett. **61**, 2689 (1988).

[47](a) A. G. Whittaker, Nature **276**, 695 (1978); Science **200**, 763 (1978); **229**, 485 (1985); (b) R. B. Heimann, J. Kleinman, and N. M. Salansky, Nature **306**, 164 (1983).

[48]D. A. Bochvar, M. V. Nikerov, and I. V. Stankevich, Sov. Sci. Rev. Chem. B **9**, 483 (1987), and references therein.

[49]P. P. K. Smith and P. R. Buseck, Science **216**, 985 (1982); **229**, 487 (1985).

[50]S. Nosé, Mol. Phys. **52**, 255 (1984); J. Chem. Phys. **81**, 511 (1984); W. Hoover, Phys. Rev. A **31**, 1695 (1985).

[51]G. B. Bachelet, D. Hamman, and M. Schluter, Phys. Rev. B **26**, 4199 (1982).

[52]L. Kleinman and D. M. Bylander, Phys. Rev. Lett. **48**, 1425 (1982).

[53]$g(r)=\sum_{i,j} g_{ij}(r)$ where $i,j=3,4$ for a-C and $i,j=2,3,4$ for l-C. g_{ij} is defined to be the number of particles with coordination i per unit volume, found at a distance r from an origin site with coordination j.

[54]D. J. Chadi, J. Vac. Sci. Technol. A **2**, 948 (1984).

[55]J. Robertson, Philos. Mag. B **47**, L33 (1983).

[56]C. A. Coulson, in *Valence* (Oxford Clarendon, Oxford, England, 1958), Chap. VIII.

[57]A. Karpfen, J. Phys. C **12**, 3227 (1979); M. J. Rice, A. R. Bishop, and D. K. Campbell, Phys. Rev. Lett. **51**, 2136 (1983).

[58]See, e.g., D. J. Thouless, Phys. Rep. **13**, 93 (1974).

[59]See, e.g., N. F. Mott, Philos. Mag. **19**, 30 (1969).

[60]Our investigation of high pressure ($P\simeq 1$ Mbar) l-C [G. Galli, R. M. Martin, R. Car, and M. Parrinello (unpublished)] shows that the system has structural and bonding properties remarkably different from those of the low-P liquid.

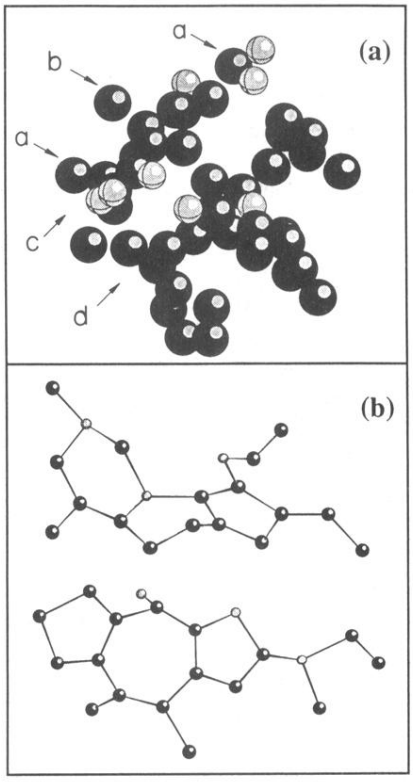

FIG. 5. Microscopic structure of the computer-generated *a*-C network: (a) the entire set of atoms belonging to one MD cell and (b) several fivefold, sixfold, and sevenfold ring structures the system is composed of are displayed (see text). Black and grey spheres indicate threefold and fourfold coordinate atoms, respectively.

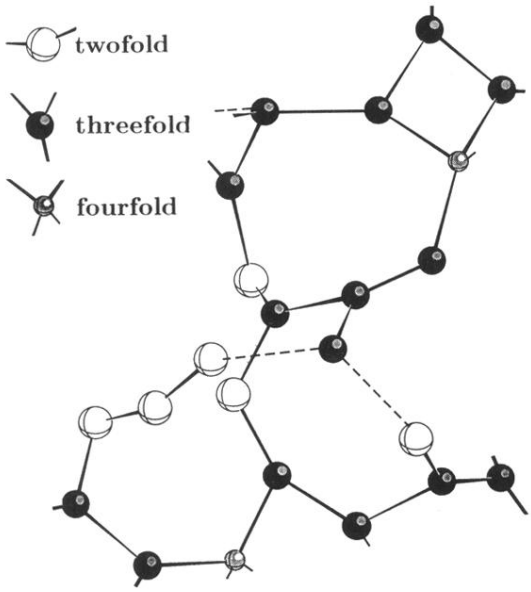

FIG. 9. Several atoms of a representative configuration of *l*-C are displayed (see text). White, black, and grey spheres indicate twofold, threefold, and fourfold coordinated atoms, respectively. Bonds with length close to the first minimum of the correlation function $g(r)$ (see Fig. 2) have been represented as dotted lines.